Journal of Coordination Chemistry
Publication details, including instructions for authors and subscription information:
http://www.tandfonline.com/loi/gcoo20

Assembly of three binuclear complexes of Ag^{I} with 2,3-bis(2-pyridyl)pyrazine and benzoyltrifluoroacetonate ligands

Farzin Marandi [a], Afsaneh Marandi [b], Mohammad Ghadermazi [b], Harald Krautscheid [c] & Mohammad Rafiee [d]

[a] Department of Chemistry, Payame Noor University, 19395-3697 Tehran, I.R. of IRAN

[b] Department of Chemistry, Faculty of Science, University of Kurdistan, Sanandaj, Iran

[c] Institut für Anorganische Chemie, Universität Leipzig, Leipzig, Germany

[d] Department of Chemistry, Institute for Advanced Studies in Basic Sciences (IASBS), Gavazang, Zanjan, Iran

Published online: 09 May 2012.

To cite this article: Farzin Marandi, Afsaneh Marandi, Mohammad Ghadermazi, Harald Krautscheid & Mohammad Rafiee (2012) Assembly of three binuclear complexes of Ag^{I} with 2,3-bis(2-pyridyl)pyrazine and benzoyltrifluoroacetonate ligands, Journal of Coordination Chemistry, 65:11, 1882-1891, DOI: 10.1080/00958972.2012.683867

To link to this article: http://dx.doi.org/10.1080/00958972.2012.683867

Journal of Coordination Chemistry
Vol. 65, No. 11, 10 June 2012, 1882–1891

Assembly of three binuclear complexes of Ag^{I} with 2,3-bis(2-pyridyl)pyrazine and benzoyltrifluoroacetonate ligands

FARZIN MARANDI*†, AFSANEH MARANDI‡, MOHAMMAD GHADERMAZI‡, HARALD KRAUTSCHEID§ and MOHAMMAD RAFIEE¶

†Department of Chemistry, Payame Noor University, 19395-3697 Tehran, I.R. of IRAN
‡Department of Chemistry, Faculty of Science, University of Kurdistan, Sanandaj, Iran
§Institut für Anorganische Chemie, Universität Leipzig, Leipzig, Germany
¶Department of Chemistry, Institute for Advanced Studies in Basic Sciences (IASBS), Gavazang, Zanjan, Iran

(*Received 1 December 2011; in final form 8 February 2012*)

Three binuclear Ag^{I} complexes based on β-diketonate and N-donor ligands, $[Ag_2(2,3\text{-bpp})_2(btfa)_2]$ (**1**) and $[Ag_2(2,3\text{-bpp})_2(cbtfa)_2]$ (**2**), and $[Ag_2(2,3\text{-bpp})_2(mbtfa)_2]$ (**3**), where 2,3-bpp is 2,3-bis(2-pyridyl)pyrazine, Hbtfa is benzoyltrifluoroacetone, Hcbtfa is 4-chlorobenzoyltrifluoroacetone, and Hmbtfa is 4-methoxybenzoyltrifluoroacetone, were prepared and characterized by elemental analysis, IR, and ^{1}H NMR spectroscopy and X-ray crystallography. Thermal and electrochemical properties were also studied. The complexes are structurally quite similar. Three nitrogen atoms of 2,3-bpp in **1**, **2**, and **3** are donors toward two silver(I) ions in syn-conformation. Abundant weak interactions, such as $\pi\cdots\pi$, C–H$\cdots$F, and C–H$\cdots$O interactions, provide additional assembly forces, leading to 3-D supramolecular networks for **1**–**3**.

Keywords: Ag^{I}; β-Diketonate; 2,3-bis(2-pyridyl)pyrazine

1. Introduction

Polydentate nitrogen heterocycles have played considerable roles in coordination chemistry and crystal engineering because of their good coordinating properties and their ability to transmit electronic effects [1–4]. One example is 2,3-bis(2-pyridyl)pyrazine (2,3-bpp), a bis-a-diimine type ligand with four nitrogen donors binding to two metal centers simultaneously like 2,2′-bipyrimidine (bpm) but with greater flexibility. Accordingly, 2,3-bpp based complexes containing Ru^{2+}, Ir^{3+}, Os^{2+}, Pt^{2+}, Rh^{3+}, Cu^{2+}, Ni^{2+}, Cd^{2+}, Re^{+}, etc. have fascinating topological geometries and interesting properties [5–7]. However, by comparison, its silver(I) coordination chemistry has not been extensively explored [8]. Our interest focuses on the d^{10} metal-based 2,3-bpp complexes for self-assemblies of metal–organic coordinations and supramolecular architectures.

*Corresponding author. Email: fmarandi2004@yahoo.com

ISSN 0095-8972 print/ISSN 1029-0389 online
http://dx.doi.org/10.1080/00958972.2012.683867

Some control over the type and topology of the product generated from self-assembly of inorganic metal species and organic ligands can be achieved by careful choice of the building blocks (metal complex and organic ligand), solvent system or metal-to-ligand ratio [9]. The use of unsaturated transition-metal coordination complexes and organic bidentate or multifunctional ligands as precursors to organic–inorganic hybrid materials is of considerable interest due to diverse architectures and the potential properties of these materials, such as magnetic, nonlinear optical, catalysis, electronic properties, and as suitable precursors for preparation of nano-scale materials [10]. In contrast, unsaturated metal complexes of β-diketonates are of interest as building blocks of supramolecular structures. Several crystalline products have been synthesized by using [M(β-diketonato)$_2$] complexes (M = Pb, Cd) and different bridging and chelating ligands [11]. In particular, research has concentrated on use of 2,3-bis(2-pyridyl)pyrazine and fluorinated β-diketonate anions for synthesis, crystal structures, thermogravimetric, and cyclic voltammetric properties of new silver(I) compounds.

2. Experimental

2.1. *Materials and physical measurements*

All reagents purchased commercially were used without further purification. Infrared spectra were recorded as KBr pellets using Perkin–Elmer 597 and Nicolet 510 P spectrophotometers. Elemental analyses (C, H, and N) were performed using a Carlo ERBA model EA 1108 analyzer. Solution ^{1}H NMR spectra were recorded on a BRUKER DRX-500 AVANCE spectrometer at 500 MHz using d_6-DMSO. Thermal analyses were carried out on a Seiko Instruments thermal analyzer. Cyclic voltammetry was performed using an Autolab potentiostat/galvanostat 101. The working electrode was a glassy carbon disk (2.0 mm diameter) with a Pt wire as counter electrode. The working electrode potentials were measured *versus* a quasi-reference electrode of a platinum wire (all electrodes from Azar Electrode).

2.2. *Crystallography*

Single crystal X-ray diffraction data of **1**, **2**, and **3** were collected on imaging plate diffractometers IPDS-1 at 213 K and IPDS-2T at 180 K, respectively (Stoe & Cie GmbH, Darmstadt, Germany), using Mo-Kα radiation ($\lambda = 71.073$ pm). The data reductions were performed using the STOE X-AREA software package [12]. The structures were solved by direct methods using SHELXS-97 and refined by full-matrix least-squares based on F^2 using SHELXL-97 [13]. Anisotropic displacement parameters were used for Ag, C, Cl, F, N, and O; disordered fluorine atoms (**1**) were refined with isotropic displacement parameters, hydrogen atoms were included in calculated positions. The basic crystallographic data of **1**–**3** are summarized in table 1. Graphical presentations were drawn using ORTEP-3 [14].

2.3. *Preparation of [Ag_2(2,3-bpp)$_2$(btfa)$_2$] (1)*

A mixture of Ag_2O (116 mg, 0.5 mmol), 2,3-bpp (0.234 g, 1.0 mmol) and Hbtfa (216 mg, 1 mmol) was stirred in CH_3CN/H_2O (15 mL, v/v: 1/1). Then, an aqueous NH_3 solution

Table 1. Crystal data and structure refinement for **1–3**.

	1	**2**	**3**
Identification code	$[Ag(bppz)(btfa)]_2$	$[Ag(bppz)(Clbtfa)]_2$	$[Ag(bppz)(mbtfa)]_2$
Empirical formula	$C_{48}H_{32}Ag_2F_6N_8O_4$	$C_{48}H_{30}Ag_2Cl_2F_6N_8O_4$	$C_{50}H_{30}Ag_2F_6N_8O_6$
Formula weight	1114.56	1183.44	1174.61
Crystal system	Triclinic	Triclinic	Triclinic
Space group	$P\bar{1}$	$P\bar{1}$	$P\bar{1}$
Unit cell dimensions (Å,°)			
a	9.1191(8)	9.1124(11)	9.3092(10)
b	9.3389(8)	9.4865(10)	9.4349(9)
c	14.6847(11)	15.3338(19)	15.7462(14)
α	92.768(9)	97.813(9)	100.379(7)
β	93.901(10)	90.686(9)	90.957(8)
γ	116.332(9)	116.831(8)	118.072(7)
Volume (Å^3), Z	1113.91(16), 1	1167.8(2), 1	1192.1(2), 1
Calculated density (g cm^{-3})	1.649	1.683	1.636
Absorption coefficient (mm^{-1})	0.959	1.013	0.904
$F(000)$	548	588	588
θ range for data collection (°)	2.5–27.0	2.4–27.0	2.5–27.0
Limiting indices	$-11 \le h \le 11$; $-11 \le k \le 11$; $-18 \le l \le 18$	$-10 \le h \le 11$; $-12 \le k \le 12$; $-19 \le l \le 19$	$-11 \le h \le 11$; $-12 \le k \le 12$; $-20 \le l \le 20$
Reflections collected	10421	12890	15655
Independent reflections	4529 [R(int) = 0.0291]	5118 [R(int) = 0.0496]	5207 [R(int) = 0.0422]
Completeness to θ (%)	93.1	100.0	100.0
Data/restraints/parameters	4529/0/307	5118/0/317	5207/0/336
Goodness-of-fit on F^2	0.971	0.847	0.976
Final R indices [$I > 2\sigma(I)$]	$R_1 = 0.0320$	$R_1 = 0.0329$	$R_1 = 0.0351$
Final R indices (all data)	$wR_2 = 0.0867$	$wR_2 = 0.0649$	$wR_2 = 0.0789$
Largest difference peak hole (e Å^{-3})	0.89 and −0.61	0.60 and −0.76	0.66 and −0.67

(25%) was poured into the mixture to give a clear solution. The resulting solution was allowed to evaporate slowly in the dark at room temperature for several days to give colorless crystals of **1**. The crystals were washed with a small volume of cold methanol and diethyl ether. Anal. Calcd for $C_{48}H_{32}Ag_2F_6N_8O_4$: C, 51.68; H, 2.87; N, 10.05. Found (%): C, 52.07; H, 2.58; N, 10.27. IR (KBr, cm^{-1}): 3085(m), 1625(s), 1610(s), 1605(s), 1590(s), 1515(s), 1473(s), 1348(m), 1316(m), 1248, 1143, 1025(m), 767(m), 649(w), ^{1}H NMR (DMSO, δ): 8.79 (d, 2H, pyrazine), 8.38 (m, 2H, pyridyl), 7.90 (m, 2H, pyridyl), 7.7–7.8 (m, 4H, pyridyl, and phenyl), 7.3–7.5 (m, 5H, pyridyl and phenyl), 5.91 (s, 1H, =CH– of btfa$^-$).

2.4. *Preparation of [Ag_2(2,3-bpp)$_2$(cbtfa)$_2$] (2)*

Complex **2** was synthesized as for **1** using Hcbtfa (250 mg, 1 mmol) in place of Hbtfa. Anal. Calcd for $C_{48}H_{30}Ag_2Cl_2F_6N_8O_4$: C, 48.67; H, 2.53; N, 9.46. Found (%): C, 48.37; H, 2.23; N, 9.57. IR (KBr, cm^{-1}): 3075(m), 1635(s), 1615(m), 1607(s), 1585(s), 1520(s), 1495(s), 1352(m), 1256, 1194, 1142(m), 1045(m), 1024(m), 785(m), 666(w). ^{1}H NMR (DMSO, δ): 8.77 (d, 2H, pyrazine), 8.38 (d, 2H, pyridyl), 7.7–8.0 (m, 4H, pyridyl and phenyl), 7.3–7.6 (m, 4H, pyridyl, and phenyl), 5.86 (s, 1H, =CH– of cbtfa$^-$).

2.5. *Preparation of [Ag_2(2,3-bpp)$_2$(mbtfa)$_2$] (3)*

Complex **3** was synthesized in the same way as **1** using Hmbtfa (208 mg, 1 mmol) in place of Hbtfa. Anal. Calcd for $C_{50}H_{36}Ag_2F_6N_8O_6$: C, 51.08; H, 3.06; N, 9.53. Found (%): C, 50.87; H, 3.26; N, 9.41. IR (KBr) m (cm^{-1}): 3044(m), 2956(m), 1620(s), 1613(m), 1610(s), 1575(s), 1515(s), 1492(s), 1349(m), 1266, 1205, 1140(m), 1048(m), 1026(m), 780(m), 666(w). ^{1}H NMR (DMSO, δ): 8.78 (d, 4H, pyrazine), 8.36 (d, 4H, pyridyl), 7.7–8.0 (m, m, 5H, pyridyl, and phenyl), 7.38 (d, 2H, pyridyl), 6.92 (d, 2H, phenyl), 5.90 (s, 1H, = CH– of mbtfa$^-$), 3.75 (s, 3H, methoxy).

3. Results and discussion

3.1. *Synthesis, spectroscopic studies, thermogravimetry, and cyclic voltammetry*

The conventional solution reaction between silver(I) oxide and benzoyltrifluoroacetone ligands with 2,3-bis(2-pyridyl)pyrazine in CH_3CN–H_2O yielded crystalline materials formulated as [Ag_2(2,3-bpp)$_2$(btfa)$_2$] (**1**), [Ag_2(2,3-bpp)$_2$(cbtfa)$_2$] (**2**), and [Ag_2(2,3-bpp)$_2$(mbtfa)$_2$] (**3**).

IR spectra display characteristic absorptions for 2,3-bpp and β-diketonates. The relatively weak absorptions at 3085, 3075, and 3044 cm^{-1} are due to C–H ring hydrogen atoms in **1**, **2**, and **3**, respectively, and 2956 cm^{-1} due to C–H of the methoxy group of the mbtfa$^-$ in **3**. In IR spectra of **1**, **2**, and **3**, shift toward higher wavenumbers of the characteristic peaks of pyrazine [1605, 1607, 1610 and 1610, 1615, 1613 cm^{-1} (**1**, **2**, and **3**) *versus* 1563 and 1580 cm^{-1} (free ligand)] and pyridine [1025, 1024, 1026 and 1043, 1045, 1048 cm^{-1} (**1**, **2**, and **3**) *versus* 991 cm^{-1} (free ligand)] are indicative of coordination of 2,3-bpp [15]. The aromatic ring vibrations of 2,3-bpp in **1**, **2**, and **3** at 1600–1350 cm^{-1} are somewhat shifted to higher wavenumbers in comparison to free 2,3-bpp, as expected upon metal coordination [16]. IR spectra of the complexes show strong bands at 1625, 1635, 1620 cm^{-1} and at 1515, 1520, 1515 cm^{-1}, assigned to the ν(C = O) and ν(C = C) stretches of β-diketonates. These bands are at significantly lower energies than those for free Hbtfa, Hcbtfa, Hmbtfa (1675, 1686, 1676 cm^{-1}) and are indicative of β-diketonate chelation to Ag^I. The absorption bands at 1260–1130 cm^{-1} correspond to C–F modes of the β-diketonates [17].

^{1}H NMR spectra of DMSO solutions of **1**, **2**, and **3** display separated five peak for protons of 2,3-bpp at 7.4–8.8 ppm (also seen in coordination of 2,3-bpp in a syn-conformation [18]) and singlets at 5.91, 5.86, and 5.90 ppm of = CH– protons of btfa$^-$, cbtfa$^-$, and mbtfa$^-$ anions, respectively. In **1** (three distinct peaks of the phenyl group), **2** (two distinct peaks of the 4-chlorophenyl group), and **3** (two distinct peaks of the 4-methoxyphenyl group) β-diketonates appear at 7.3–7.8 ppm (overlapped with protons of 2,3-bpp) for **1** and **2** and 6.92 and 7.7–8.0 ppm (the peaks overlapped with protons of 2,3-bpp) for **3**. The singlet at 3.75 ppm was assigned to the three protons of the methoxy group in mbtfa$^-$.

The thermogravimetry curves show that **1**, **2**, and **3** exhibit similar decomposition pathways. No weight loss is observed to 200°C demonstrating that **1**, **2**, and **3** are retained to these temperatures. Thermal decomposition of the compounds occurs in one step at 200–300°C (almost 80% weight). The mass loss calculations as well as microanalyses of the solid residues suggest that the residue left as a final decomposition

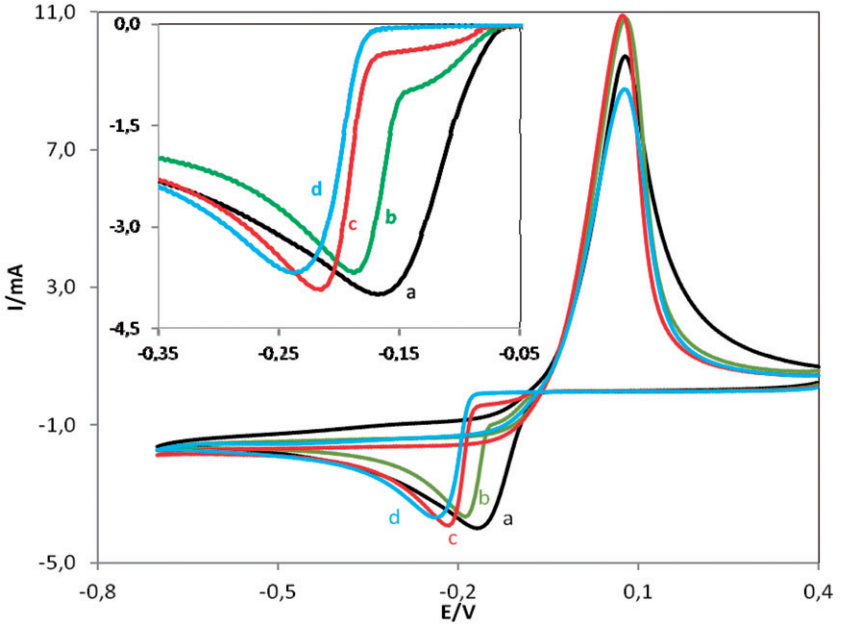

Figure 1. (I) Cyclic voltammograms of 1.0 mmol L^{-1} (a) $AgNO_3$, (b) **1**, (c) **2,** and (d) **3** at glassy carbon electrode in DMSO, supporting electrolyte 0.1 mol L^{-1} TBAP and scan rate 100 mV s^{-1}. Inset: expansion of cathodic peaks.

product is Ag_2O and the remaining mass of 21.50% for **1** (Calcd 20.82%), 20.80% for **2** (Calcd 19.60%) and 20.50% for **3** (Calcd 19.75%), respectively, agrees with expected values.

Voltammetric studies of **1**, **2**, and **3** were performed in DMSO containing 0.1 mol L^{-1} tetrabutylammonium perchlorate. Figure 1 (curve a) shows the cyclic voltammogram (CV) of $AgNO_3$ in DMSO; curves (b) to (d) are the CVs of **1**, **2**, and **3** at the same conditions. All the CV exhibit one cathodic peak in the negative scan and a corresponding anodic peak in the positive scan. The cathodic peaks are due to reduction of Ag^+ and the anodic peaks are related to oxidation of Ag deposited on the electrode surface. As shown in this figure, the cathodic peak potential of the complexes shifts to more negative values (−36 mV, −53 mV, and −73 mV for **1**, **2**, and **3**, respectively), which indicates stability of silver ions in complexes. Considering the strong interaction of DMSO as solvent with silver ions, more negative peak potentials for the complexes are related to the higher stability of the complexes [19]. Based on these results the order of stability for the complexes is **3** > **2** > **1**. Also, the time dependent voltammetric study of the complexes shows that they have good kinetic stability.

3.2. *Description of the crystal structures of 1, 2, and 3*

Single crystal X-ray diffraction analysis reveals that the complexes form discrete neutral metallacycles [Ag(2,3-bpp)(β-diketonate)]$_2$, consisting of two 2,3-bpp, two β-diketonates, and two Ag^+ ions (figure 2), which represents the smallest 2-D cyclic assembly

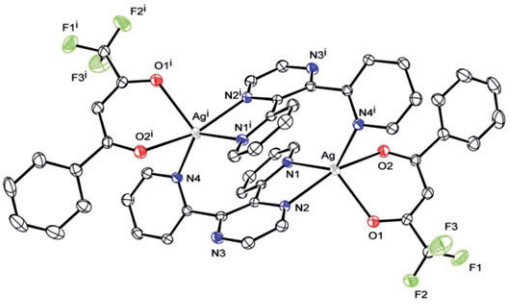

1

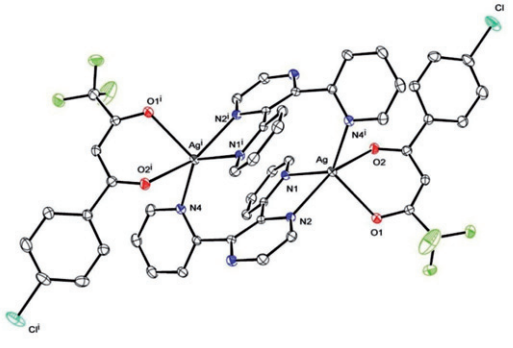

2

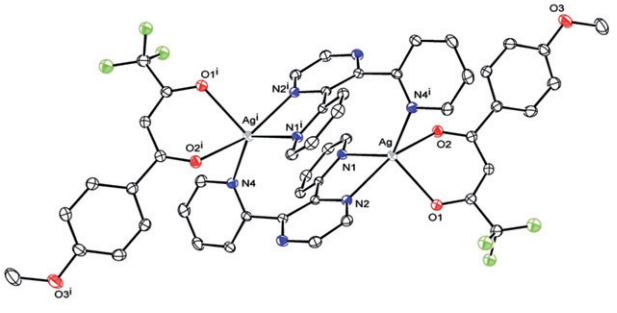

3

Figure 2. ORTEP view of **1**, **2**, and **3**. Displacement ellipsoids are shown at the 40 % probability level.

possible for closed structures with a 1 : 1 metal-to-ligand ratio. The two 2,3-bpp ligands are face-to-face in syn-conformation [18] from opposite directions to coordinate to two Ag^+ ions; each Ag^+ is five-coordinate by three nitrogen atoms (N1, N2, and $N4^i$) from two different 2,3-bpp and two oxygen atoms (O1 and O2) of one β-diketonate ($btfa^-$, $cbtfa^-$, and $mbtfa^-$) with the coordination geometry of a distorted square pyramid. The Ag–O distances range from 2.448 to 2.512 Å and the Ag–N distances from 2.298 to 2.422 Å (table 2).

The neutral $[Ag(2,3\text{-bpp})(\beta\text{-diketonate})]_2$ motif has a centre of inversion between the two Ag^+ ions. This leads to a typical rectangular cavity enclosed *via* two ligands and

Table 2. Selected bond lengths (Å) and angles (°) for **1–3**.

	1	2	3
Ag–N4^{i}	2.313(3)	2.298(2)	2.313(2)
Ag–N2	2.372(3)	2.386(2)	2.370(2)
Ag–N1	2.406(3)	2.396(2)	2.422(2)
Ag–O1	2.448(2)	2.464(2)	2.472(2)
Ag–O2	2.497(3)	2.512(2)	2.460(2)
N4^{i}–Ag–N2	123.82(9)	128.47(8)	125.61(9)
N4^{i}–Ag–N1	124.37(8)	125.83(8)	126.58(8)
N2–Ag–N1	69.85(9)	70.03(8)	70.27(8)
N4^{i}–Ag–O1	115.62(8)	117.46(8)	117.05(8)
N2–Ag–O1	91.09(8)	88.04(7)	88.07(8)
N1–Ag–O1	117.69(8)	112.99(8)	113.79(8)
N4^{i}–Ag–O2	82.33(9)	82.23(8)	82.91(8)
N2–Ag–O2	153.84(8)	149.28(8)	151.38(8)
N1–Ag–O2	97.16(8)	93.90(7)	95.52(8)
O1–Ag–O2	74.60(8)	74.03(7)	74.82(7)

^{i} $-x, -y, -z$.

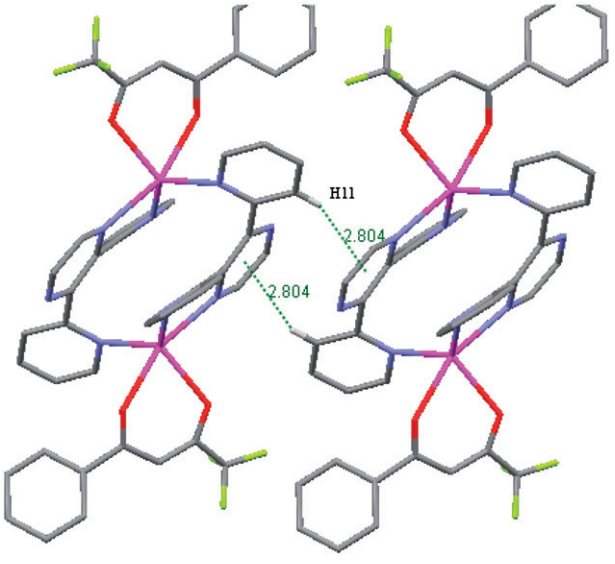

Figure 3. Packing diagram of **1**, view along [100], showing C–H···π interactions.

two Ag^{+} ions with a Ag···Ag separation of 5.346 Å for **1**, 5.196 Å for **2**, and 5.215 Å for **3**, as shown in figure 2.

Weak directional intermolecular and π–π stacking interactions have an important role in constructing the supramolecular network of these compounds.

An inspection of the data of **1**, **2**, and **3** for weak directional intermolecular interactions by MERCURY [20], which were used for O···H–C and F···H–C interactions [11] (table 3). In addition, there are C–H···π interactions among the weak interactions (figure 3, table 3), relatively strong interactions within this class of weak non-covalent contacts [21]. The packing diagram of **1** (figure 4) exhibits a 2-D

Table 3. Intermolecular interactions for **1–3**.

A···H–B	A···H (Å)	A···B (Å)	A···H–B (°)
1			
O2···H8–C8 ($-1+x$, $-1+y$, z)	2.461	3.399	175.45
O1···H3–C3 ($-x$, $1-y$, $1-z$)	2.664	3.470	144.11
O2···H3–C3 ($-x$, $1-y$, $1-z$)	2.654	3.416	138.50
N2···H11–C11 ($1-x$, $2-y$, $1-z$)	2.733	3.484	137.47
O1···H12–C12 ($1-x$, $2-y$, $1-z$)	2.582	3.412	147.33
F2···H12–C12 ($1-x$, $2-y$, $1-z$)	2.537	3.150	123.04
π–π stacking (slipped face-to-face)		3.370	
H9···Cg (C19···C24) ($1+x$, $1+y$, z)		2.708	
H11···Cg (N3···C8) ($1-x$, $2-y$, $1-z$)		2.804	
2			
O1···H3–C3 ($-x$, $1-y$, $1-z$)	2.597	3.411	144.03
O2···H3–C3 ($-x$, $1-y$, $1-z$)	2.612	3.373	137.49
O2···H8–C8 ($-1+x$, $-1+y$, z)	2.443	3.390	175.74
O1···H12–C12 ($1-x$, $2-y$, $1-z$)	2.646	3.442	141.65
F1···H20–C20 ($-x$, $1-$y, $2-z$)	2.589	3.521	166.78
F3···H21–C21 ($1+x$, $1+y$, z)	2.601	3.153	117.42
Cl···H14–C14 ($-x$, $-y$, $1-z$)	2.992	3.631	125.84
Cl···H17–C17 ($-x$, $-y$, $2-z$)	3.039	3.858	145.20
Cl···F1 ($-x$, $-$y, $2-z$)		3.244	
π–π stacking (slipped face-to-face)		3.370	
H11···Cg (N2···C6) ($1-x$, $2-y$, $1-z$)		2.695	
3			
O2···H8–C8 ($-1+x$, $-1+$y, z)	2.419	3.369	177.61
O1···H3–C3 ($-x$, $1-y$, $1-z$)	2.654	3.461	143.04
O2···H3–C3 ($-x$, $1-y$, $1-z$)	2.695	3.491	141.65
O1···H12–C12 ($1-x$, $2-y$, $1-z$)	2.632	3.427	141.49
F1A···H20–C20 ($-x$, $1-y$, $2-z$)	2.502	3.305	142.24
F3A···H21–C21 ($1+x$, $1+y$, z)	2.449	3.012	117.86
F3A···H25A–C25 ($1+x$, $1+y$, z)	2.529	3.444	155.34
H25C···Cg (C19···C24) ($-x$, $-y$, $2-z$)		2.830	
π–π stacking (slipped face-to-face)		3.402	

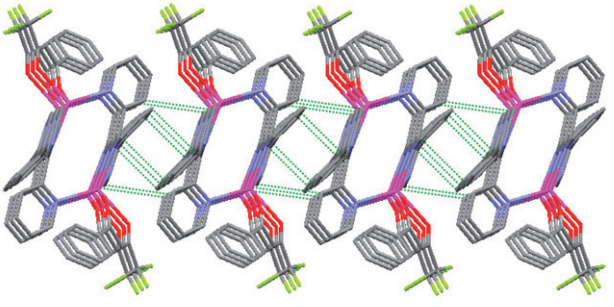

Figure 4. A part of the 2-D network of **1** viewed along the [010] plane, generated from $\pi\cdots\pi$ stacking interactions.

selfassembled structure through $\pi\cdots\pi$ stacking (slipped face-to-face) with 3.370 Å distance between the pyridine rings, shorter than for normal $\pi\cdots\pi$ stacking [22]. In addition to $\pi\cdots\pi$ stacking, in **2** and **3**, 3-D supramolecular networks are constructed by

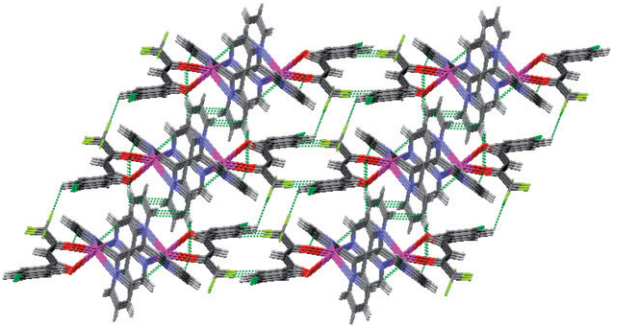

Figure 5. A part of the 3-D network of **2** viewed along [010], generated from intermolecular interactions (table 3).

O···H–C and F···H–C interactions that are substantially shorter than the van der Waals distances of 2.77 Å for O, H and 2.67 Å for H, F distance [23] (figure 5).

A useful comparison to **1**, **2**, and **3** is provided by a recent structural study of dinuclear complexes of Ag^+ with nitrate [18]. Average Ag–N distances in **1**, **2**, and **3** are longer than in $[Ag(2,3\text{-bpp})(NO_3)]_2$, and two aryl ring planes of 2,3-bpp (plane of pyridyl and prazine) form angles of 55.18, 55.28, and 56.34° for **1**, **2**, and **3**, respectively, more than for $[Ag(2,3\text{-bpp})(NO_3)]_2$ (47.53°). It seems reasonable to assume that differences in the dihedral angles between the aryl ring planes of 2,3-bpp coordinating to Ag^+ result from the network of directed intermolecular interactions and coordination of the anions.

4. Conclusions

We have prepared three new binuclear complexes based on 2,3-bis(2-pyridyl)pyrazine, derivatives of benzoyltrifluorocetonate and silver ions. The crystal structures are isomorphous. The three nitrogen atoms of 2,3-bpp are donors toward two Ag^+ ions in syn-conformation. Weak interactions, such as $\pi\cdots\pi$, C–H···F and C–H···O between ligands of binuclear complexes, provide additional assembly forces, leading to 3-D supramolecular networks for **1**–**3**.

Supplementary material

Full crystallographic data, in CIF format, may be obtained free of charge from the Cambridge Crystallographic Data Centre (CCDC 850256 for **1**, 850257 for **2** and 850258 for **3**) *via* www.ccdc.cam.ac.uk/cgi-bin/catreq.cgi.

Acknowledgments

Support of this investigation by Payame Noor University and Iran National Science Foundation, INSF, is gratefully acknowledged by FM.

References

[1] R. Miao, M.T. Mongelli, D.F. Zigler, B.S.J. Winkel, K.J. Brewer. *Inorg. Chem.*, **45**, 10413 (2006).
[2] S. Campagna, C. Di Pietro, F. Loiseau, B. Maubert, N. McClenaghan, R. Passalacqua, F. Puntoriero, V. Ricevuto, S. Serroni. *Coord. Chem. Rev.*, **229**, 67 (2002).
[3] A.A. Holder, D.F. Zigler, T.M. Tarrago-Trani, B. Storrie, K.J. Brewer. *Inorg. Chem.*, **46**, 4760 (2007).
[4] F. Puntoriero, F. Nastasi, M. Cavazzini, S. Quici, S. Campagna. *Coord. Chem. Rev.*, **25**, 536 (2007).
[5] (a) R.R. Ruminski, K.D.K. Zimmer, K.A. Rita, M.A. Knobbe, C. Dean. *Inorg. Chim. Acta*, **362**, 1772 (2009); (b) F.S. Delgado, F. Lahoz, F. Lloret, M. Julve, C. Ruiz-Perez. *Cryst. Growth Des.*, **8**, 3219 (2008).
[6] (a) K. Ha. *Acta Crystallogr. Sect. E: Struct. Rep. Online*, **67**, m1454 (2011); (b) A. Jain, C. Slebodnick, B.S.J. Winkel, K.J. Brewer. *J. Inorg. Biochem.*, **102**, 1854 (2008); (c) S.M. Arachchige, K.J. Brewer. *Inorg. Chem. Commun.*, **10**, 1159 (2007); (d) F. Kennedy, N.M. Shavaleev, T. Koullourou, Z.R. Bell, J.C. Jeffery, S. Faulkner, M.D. Ward. *Dalton Trans.*, 1492 (2007).
[7] (a) J.M.D. Zapiter, B.M. Tissue, K.J. Brewer. *J. Coord. Chem.*, **64**, 3366 (2011); (b) Q. Gao, Y.-B. Xie, S. Chen, D. Wang. *J. Chem. Crystallogr.*, **37**, 797 (2007). (c) M. Newell, J.A. Thomas. *Dalton Trans.*, 705 (2006).
[8] L. Cunha-Silva, R. Ahmad, M.J. Carr, A. Franken, J.D. Kennedy, M.J. Hardie. *Cryst. Growth Des.*, **7**, 658 (2007).
[9] (a) O.S. Jung, S.H. Park, K.M. Kim, H.G. Jang. *Inorg. Chem.*, **37**, 5781 (1998); (b) T.L. Hennigar, D.C. MacQuarrie, P. Losier, R.D. Rogers, M.J. Zaworotko. *Angew. Chem. Int. Ed. Engl.*, **36**, 972 (1997).
[10] (a) L. Brammer. *Chem. Soc. Rev.*, **33**, 476 (2004); (b) S. Kitagawa, R. Kitaura, S. Noro. *Angew. Chem. Int. Ed.*, **43**, 2334 (2004); (c) R. Bashiri, K. Akhbari, A. Morsali. *Inorg. Chim. Acta*, **362**, 1035 (2009); (d) K. Akhbari, A. Morsali, P. Retailleau. *Polyhedron*, **29**, 3304 (2010); (e) K. Akhbari, A. Morsali. *CrystEngComm*, **12**, 3394 (2010); (f) Z. Rashidi Ranjbar, A. Morsali. *Synth. Met.*, **161**, 1449 (2011).
[11] F. Marandi, Z. Nikpey, M. Khosravi, H.-K. Fun, M. Hemamalini. *J. Coord. Chem.*, **64**, 3012 (2011), and references therein.
[12] *X-AREA*. Stoe & Cie Darmstadt, Germany (2006).
[13] G.M. Sheldrick. *Acta Cryst.*, **A64**, 112 (2008).
[14] L.J. Farrugia. *J. Appl. Crystallogr.*, **30**, 565 (1997).
[15] H.D. Stidham, J.V. Tucci. *Spectrochim. Acta Part A*, **23**, 2233 (1962).
[16] J. Carranza, H. Grove, J. Sletten, F. Lloret, M. Julve, P.E. Kruger, C. Eller, D.P. Rillema. *Eur. J. Inorg. Chem.*, 4836 (2004).
[17] S. Bureekaew, S. Horike, M. Higuchi, M. Mizuno, T. Kawamura, D. Tanaka, N. Yanai, S. Kitagawa. *Nat. Mater.*, **8**, 831 (2009).
[18] Z.-Y. Zhou, Y. Cai, H.-C. Fang, Q.-G. Zhan, H.-J. Jin, Y.-H. Feng, Y.-P. Cai. *Inorg. Chim. Acta*, **363**, 877 (2010).
[19] K. Izutsu. *Electrochemistry in Nonaqueous Solutions*, Wiley-VCH, Weinheim (2002).
[20] *MERCURY* (*Version1.4.1*). Copyright Cambridge Crystallographic Data Centre, 12 Union Road, Cambridge, CB2 1EZ, UK (2001–2005).
[21] F. Marandi, H.-K. Fun, C. Chantrapromma. *J. Coord. Chem.*, **62**, 2155 (2009).
[22] L. Saghatforoush, F. Marandi, I. Pantenburg, G. Meyer. *Z. Anorg. Allg. Chem.*, **635**, 1523 (2009).
[23] (a) G. Althoff, J. Ruiz, V. Rodriguez, G. Lopez, J. Perez, C. Janiak. *CrystEngComm*, **8**, 662 (2006); (b) J. Emsley. *The Elements*, Oxford University Press, Oxford (1989).